Research Article

Investigation the Effect of Encapsulated Bromelain Enzyme in Magnetic Carbon Nanotubes on Colorectal Cancer Cells

Ardalan Montazeri [1], Mina Ramezani [1, *] and Azadeh Mohammadgholi [1]

[1]Department of Biology, Faculty of Sciences, Central Tehran Branch, Islamic Azad University, Tehran, Iran

[*]*Corresponding author*: Department of Biology, Faculty of Sciences, Central Tehran Branch, Islamic Azad University, Tehran, Iran. Email: mina.ramezani@gmail.com

Abstract

Background: Bromelain (BL) is an enzyme extracted from *Ananas comosus*, which has been known for its therapeutic properties.

Objectives: The anticarcinogenic activity of BL was examined with and without the presence of magnetic carbon nanotubes (MCNTs) against HT-29 colorectal cancer cells.

Methods: The operational factors affecting BL adsorption, such as contact time (30, 60, 90, 120, and 180 min), adsorbent dosage (1 g/L and 5 g/L), initial bromelain concentration (50, 150, and 300 mg/L), and temperature (35 and 50°C) were studied in details. Then, cancer cells were exposed to various BL concentrations (0.1, 1, 10, and 100 μg/mL), and the cell viability was determined by methylthiazol tetrazolium (MTT) assay after 24, 48, and 72 h.

Results: The highest adsorption of BL on nanotubes was at 41.62 mg/L and achieved at 35°C and 90 min at the initial concentration of 50 mg/L and 1 g/L of MCNTs. The adsorption followed the Freundlich model and second-order kinetics. The results indicated that MCNTs could be a potential effective adsorbent for the removal of BL.

Conclusions: MTT assay indicated that BL at a concentration of 100 μg/mL alone and in combination with MCNTs efficiently inhibited the HT-29 cancerous cells. However, encapsulated BL had a considerable advantage of slow delivery, which is favorable for cancer treatment.

Keywords: Bromelain Enzyme, Anticarcinogenic, Cytotoxicity, Magnetic Carbon Nano-tubes, Colorectal Cancer

1. Background

Colorectal cancer is the third most common cancer worldwide and the fourth leading cause of cancer-related death (1). Bromelain (BL) is a 26 kDa proteolytic enzyme and the main component of the pineapple (2). BL may have various health benefits, such as anticancer, immunomodulatory, anti-inflammatory, and fibrinolytic activity. It is also used for skin debridement, platelet aggregation, enhancing adsorption of other drugs, and as a digestive aid (3). It was reported that BL is absorbed into the human intestine without degradation and without losing biological activity (4). The non-toxic nature of BL has made it a proper candidate for cancer treatment (5).

The anticarcinogenic activity of BL has been validated in in vivo and in vitro experiments (5). Some studies have indicated the anticancer activity of BL against breast cancer (6). It has been reported that BL can exert its effects by increasing the expression of p53 and Bax in 2-stage tumorigenesis of mouse skin. Gani et al. suggested that the pineapple juice might have anticarcinogenic effects on ovarian and colon cancer through apoptosis (2).

Nowadays, one of the common strategies in clinical cancer treatment is chemotherapy. However, these drugs have high toxicity and nonspecific distribution in the body (non-targeted directly to cancerous tissues), leading to various side effects and a lower level of patient compliance with treatment (7, 8).

Carbon nanotubes (CNTs) are long, cylindrical structures that are made from graphite sheets. Single-walled carbon nanotubes (SWCNTs) have a monolayer of carbon atoms in their structures and a diameter of about 1nm, half the diameter of a DNA helix. Due to their small size, these particles can easily cross biological membranes to reach the cell. CNTs are among the compounds that have recently received much more attention in drug delivery. CNTs can be used as carriers for carrying biological molecules, such as protein, DNA, and drugs. Medicinal compounds are loaded onto or inside these structures. The surface of these particles is functionalized with various groups and compounds to increase the solubility and biocompatibility, as well as the conductivity of different materials. Targeting and transferring two or more compounds simultaneously

are other features of interest in drug delivery (9, 10).

In this research, magnetic CNTs were used as a new method because the small size of the CNTs makes the removal process from the solution challenging. It has been recommended to use MCNTs because techniques, such as centrifuge and filtration require a great deal of time and energy. Also, MCNTs have higher stability in acidic and basic solutions as well as organic solvents (11, 12).

2. Objectives

In this study, we not only tried a nontoxic drug (BL) as an anticancerous drug but also enhanced BL efficacy via nanotechnology. In this respect, MCNTs were applied as a BL absorbent. These magnetic properties increase the targeted delivery of an anticancer drug to tumor cells by improving target cell recognition. This research was done to compare the efficacy of BL to inhibit the progression of human colorectal HT-29 cancer cells in the form of pure BL or encapsulating BL in MCNTs.

3. Methods

3.1. Materials

BL enzyme (Anaheal 500 containing 200 mg of BL) was purchased from Salamat Parmoon Amin Company, Iran. MCNTs, (3-(4,5-dimethylthiazol-2-yl)-2,5-diphenyltetrazolium bromide) (MTT), trypsin-EDTA, methanol, fetal bovine serum (FBS), 6305UV-VIS spectrophotometer from Jenway (UK), Dulbecco's Modified Eagle Medium (DMEM), penicillin, streptomycin, hydrochloric acid, and sodium hydroxide were acquired from Sigma-Aldrich (USA). The HT-29 cell line (colorectal adenocarcinoma) was bought from Pasteur Institute (Iran) and cultured in DMEM medium (containing 10% FBS) and 100 U mL^{-1} penicillin and 100 μg mL^{-1} streptomycin at 5% CO_2 pressure at 37°C in a flask (25 cm^3). The cells were then cultured in 24-well culture plates (1.5×10^5 cells per milliliter). Cell counts were performed using a hemocytometer slide.

3.2. Adsorption of BL on MCNTs

In this step, 1 g of Anaheal 500 was added to 1L of methanol to prepare the stock solution, and it was sonicated for 1 hour. In order to draw a calibration curve for spectrophotometry, diluted solution and standard solutions at concentrations of 5 to 50 mg L^{-1} were prepared. The standard absorbance values for each sample were obtained using spectrophotometry. All adsorption experiments were carried out indoors, inside 25 mL Erlenmeyer

flasks containing 10 mL of BL solution and adsorbent (MCNTs) in various concentrations, temperatures, and exposure times.

It should be noted that the range of variation of the measured parameters was determined using the optimal range chosen by other researchers (13, 14).

After stabilization of the conditions, samples were placed in a mixer at 240 rpm for proper mixing of adsorbent and adsorbed material. After a specified time, the adsorbent was separated from the solution using a magnet and nanometer filter, and residual concentrations of the solution were measured via the spectrophotometer calibration chart at the maximum absorbance wavelength of the BL (280 nm).

The pH of the solutions was adjusted using 0.1 M hydrochloric acid and 0.1 M sodium hydroxide to about 7.2 - 7.4 (7). Each test was repeated three times, and their averages were presented as the final results.

The amount of BL adsorbed on the adsorbent, and its removal efficiency were obtained using Equations 1 and 2.

$$q_e = \frac{(C_0 - C_e)}{M} V \tag{1}$$

$$Removal\ Efficiency\ (\%) = \frac{(C_0 - C_e)}{C_0} \times 100 \tag{2}$$

In Equation 1, q_e is the BL (mg) absorbed on the absorbent (g), C_e and C_0 (mg L^{-1}) are the equilibrium and initial concentrations of BL, respectively, M and V are the mass of adsorbent (g), and the volume of solution (L), respectively.

3.3. Contact Time Effect

The contact time was studied during 180 min using optimum pH (7.2 - 7.4), 50 mg L^{-1} BL, and 1 g L^{-1} adsorbent (MCNTs) at room temperature, and then equilibrium time was determined.

In order to prepare the sample solutions, 1 mg of BL and 10 mg of MCNTs were poured into 10 mL of methanol and sonicated in an ultrasonic bath for 1 hour. Then, the pH of the samples was adjusted to 7.2 - 7.4. The absorbance of BL on MCNTs was measured after 30, 60, 90, 120, and 180 min. The percentage of BL absorbed at different contact times and the optimum contact time (the maximum adsorption of the drug by the MCNTs) was obtained by drawing the diagram. It should be noted that the kinetic equations of adsorption were obtained from the results of these experiments.

3.4. Different Concentrations of BL and MCNTs

The effect of different concentrations of MCNTs (1 and 5 g L^{-1}) and BL solution (50, 150, and 300 mg L^{-1}) was studied at

the optimum pH and contact time and at 35°C. Thus, three samples were prepared with 1 g L^{-1} MCNTs and 50, 150, and 300 mg L^{-1} of BL and three samples with 5 g L^{-1} MCNTs and 50, 150, and 300 mg L^{-1} of BL, respectively. Subsequently, the equilibrium isotherms of the adsorption were investigated, as previously explained.

3.5. Temperature Effect

The adsorption process was carried out at two temperatures (35 and 50°C) to determine the optimum temperature as well as the thermodynamic study. At each temperature, three doses of BL (50, 150, and 300 mg L^{-1}) aqueous solution under optimum conditions of pH, contact time, and adsorbent concentration of 1 g L^{-1} were used. Shaker-incubator was used to adjust the temperature and mixing speed. The BL-free adsorbent with a similar concentration was used as a control. Then, the effect of temperature on the adsorption of BL on MCNTs was determined, as explained previously.

3.6. Adsorption Equilibriums

When the solid surface is in front of the adsorbent, the adsorbed molecules hit the solid surface where some molecules are attached or adsorbed to the solid surface, and the rest of the molecules return. The adsorption rate is initially high due to the vacancy of the adsorbent surface, but gradually, the adsorption rate decreases as the adsorbent surface is coated. At this time, the rate of desorption (the rate of separation of the adsorbed molecules from the adsorbent surface) increases. At the equilibrium moment, the rate of absorption equals the rate of desorption, resulting in no change in the concentration of adsorbed material on the adsorbent surface, which is a dynamic balance. In other words, the number of molecules that adhere to the surface is equal to the number of molecules that are separated from the surface.

3.7. Adsorption Isotherms

The equilibrium amounts of the adsorbed material usually increase with increasing its concentration in the solution. The relationship between the amounts of matter adsorbed per unit mass of adsorbent (q_e) in terms of equilibrium concentration absorbed in the solution (C_e) at a specific temperature is called adsorption isotherms. The most famous models used to analyze equilibrium adsorption data are Langmuir isotherm and Freundlich isotherm.

In the present study, Langmuir and Freundlich isotherm models were used to study and analyze the experimental data and to describe the equilibrium state in the adsorption between the solid and liquid phases. The Langmuir isotherm model represents a single layer and uniform adsorption of adsorbed material with the same energy on all the adsorbent surfaces. It also states that all adsorption sites have the same affinity for the adsorbent molecules, and there is no transition process of adsorbed materials on the adsorbent surface. On the other hand, in the Freundlich isotherm equation, the adsorption is considered multi-layered, non-uniform, and heterogeneous. The linear equations of the Langmuir and Freundlich equilibrium isotherms are shown in Equations 3 and 4, respectively.

$$\frac{C_e}{q_e} = \frac{1}{K_L q_{max}} + \frac{C_e}{q_{max}} \tag{3}$$

$$ln q_e = ln K_F + \frac{1}{n} ln C_e \tag{4}$$

In Equation 3, C_e is the equilibrium concentration of BL, q_e is the amount of BL absorbed at equilibrium, q_{max} is the maximum adsorption capacity, and KL (L mg^{-1}) is the Langmuir adsorption constant. KF and n are Freundlich constants dependent on the adsorption capacity and intensity, with n values less than 1 indicating weak adsorption and values between 1 to 2 and 2 to 10 indicating moderate and favorable adsorption, respectively. Parameters of n and KL are set using the slope and y-intercept of ln q_e linear graph against ln C_e, respectively.

The desirability of the adsorption process in the Langmuir model can be determined using the RL dimensionless factor shown in Equation 5.

$$R_L = \frac{1}{1 + K_L C_0} \tag{5}$$

R_L values greater than 1 indicate undesirable adsorption, equal to 1, specify linear adsorption, equal to 0 shows irreversible adsorption, and values between 0 and 1 are desirable adsorption [15].

3.8. Kinetic Models of Adsorption Systems

Two kinetic equations (pseudo-first-order and pseudo-second-order) were considered to find the best-fitted model for the experimental data.

The pseudo-first-order kinetic equation is based on the capacity of the adsorbent and is applicable when surface adsorption occurs from within a boundary layer via a diffusion mechanism [16]. The pseudo-second-order kinetic equation shows that chemical adsorption is the dominant and controlling mechanism in the process of surface adsorption, which is based on solid-phase adsorption. It also indicates that chemical adsorption is the deceleration process of surface adsorption [17].

$$ln(q_e - q_t) = ln q_e - k_1 t \tag{6}$$

$$\frac{t}{q_t} = \frac{1}{k_2 q_e{}^2} + \frac{1}{q_e} t \tag{7}$$

In Equation 6, q_e and q_t (mg g^{-1}) are the absorption capacities at equilibrium time and a given time t (min), respectively, and k_1 (min^{-1}) is the pseudo-first-order rate constant. The values of q_e and k_1 were obtained from the intercept and slope of the ln (qe-qt) linear graph versus t, respectively.

In Equation 7, k_2 (g (mg min)$^{-1}$) is the pseudo-second-order rate constant. q_e and k_2 values were calculated from the intercept and the slope of the t/qt linear graph against t, respectively.

3.9. In Vitro Cytotoxicity

The potential cytotoxicity of BL and encapsulated BL enzyme in MCNTs on HT-29 cells was evaluated by methylthiazole tetrazolium (MTT) assay using various concentrations of BL (0.1, 1, 10, and 100 μg mL^{-1}). In this method, 100 μL of culture medium containing 10000 HT-29 cells were added to 96-well plate and incubated for 24 - 72 hours. On the second day, 100 μL of pure BL solution and MCNTs containing BL with different concentrations were added to the plates and incubated for another 24 hours. Medium, untreated cultured cells and BL standard were served as the respective control. Then, 20 μL of MTT solution was added to all plates and incubated in the dark for 4 hours. Medium-containing MTT was withdrawn, and formazan crystals were dissolved in 150 μL of acidic isopropanol and incubated for 15 minutes at room temperature. Finally, the optical density (OD) of the solution was measured at 570 nm. The viability was determined as the ratio between viable treated cells against untreated control cells.

3.10. Statistical Analysis

Statistical analysis was carried out by SPSS software version 26. All the experiments were done in triplicate. Data were analyzed using one-way ANOVA, followed by the Tukey-Kramer post hoc test. The significant level was considered $P < 0.05$.

4. Results

4.1. Contact Time Effect on BL Adsorption on MCNTs

The amount of BL adsorbed on MCNTS was investigated in the initial concentration of BL (C_0 = 50 mg L^{-1}), at a temperature of 35°C, pH of 7.2 - 7.4, and 1 g L^{-1} of MCNTs (Figure 1). The adsorption capacity at 90 min was 41.62 mg g^{-1} and then rose with increasing the time from 90 to 180 min only about 0.2 mg g^{-1}. This may be due to the filling of active sites of adsorption on MCNTs or the access of drug molecules to these active sites. Therefore, 90 min was considered as the equilibrium time for further studies.

4.2. Effect of Initial BL Concentration and Amount of Adsorbent

As it is shown, by increasing the dosage of MCNTs from 1 g L^{-1} to 5 g L^{-1}, at 35°C and optimum pH (7.2 - 7.4), the adsorption efficiency increased, and the adsorption capacity decreased significantly ($P < 0.001$) (Figure 2). The results indicated that by increasing the initial concentration of BL from 50 mg L^{-1} to 300 mg L^{-1} at 1 g L^{-1} dosage of MCNTs, the adsorption efficiency decreased from 83.2 to 54.0%, while the adsorption capacity increased from 41.62 mg g^{-1} to 162.08 mg g^{-1} (Figure 3). It is clear that the rise in the amount of adsorbent is associated with higher efficiency in the removal process. This may be due to the increase of the adsorbent area, which leads the BL molecules to reach the active sites of the adsorbent without competition. On the other hand, the increase in the amount of adsorbent had a negative effect on the adsorption capacity, which was probably due to the lack of active adsorbent surfaces during the BL adsorption process.

4.3. Temperature Effect

The effect of temperature (35 and 50°C) on adsorption of BL from solution with different concentration (50, 150, and 300 mg L^{-1}) of BL was investigated at optimum pH (7.2 - 7.4), contact time of 90 min, and the adsorbent (MCNTs) concentration of 1 g L^{-1}. By increasing the temperature from 35 to 50°C at all initial concentrations of BL solution, the adsorption efficiency decreased significantly (Figure 4).

4.4. Adsorption Isotherms

The C_e/q_e parameter is presented in terms of C_e at 35 and 50°C to determine the Langmuir and Freundlich model parameters. The parameters related to the adsorption models are calculated and compared in Table 1 (CMCNTs = 1 g L^{-1} and pH 7.2 to 7.4).

The adsorption behavior on MCNTs is more consistent with the Freundlich model than the Langmuir model (Table 1). It can be seen that the values obtained for the parameter n in the Freundlich model for both temperatures are higher than 2, which represents the desired adsorption of BL onto MCNTs. The correlation coefficient for the Freundlich model is higher than 0.98, which indicates that the BL adsorption follows the Freundlich better than the Langmuir model. The maximum adsorption capacity based on the Langmuir model was 208.3 mg g^{-1}, which was obtained at 35°C. However, the values of KF at 35 and 50°C were 14.79 and 10.33, respectively, which both indicate favorable adsorption of BL onto MCNTs.
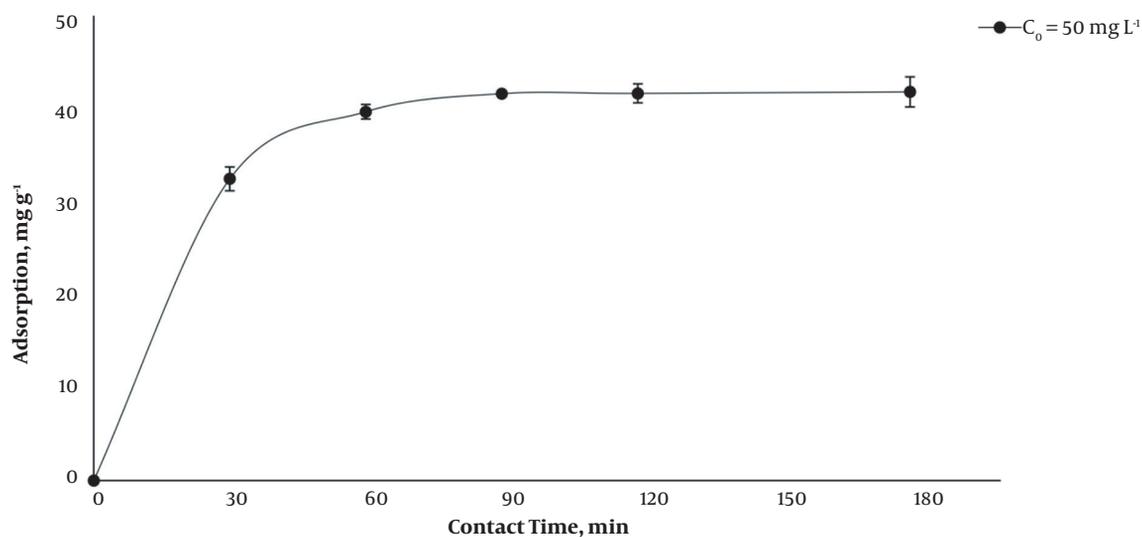
Figure 1. Effect of contact time on bromelain (BL) adsorption on magnetic carbon nanotubes (MCNTs)
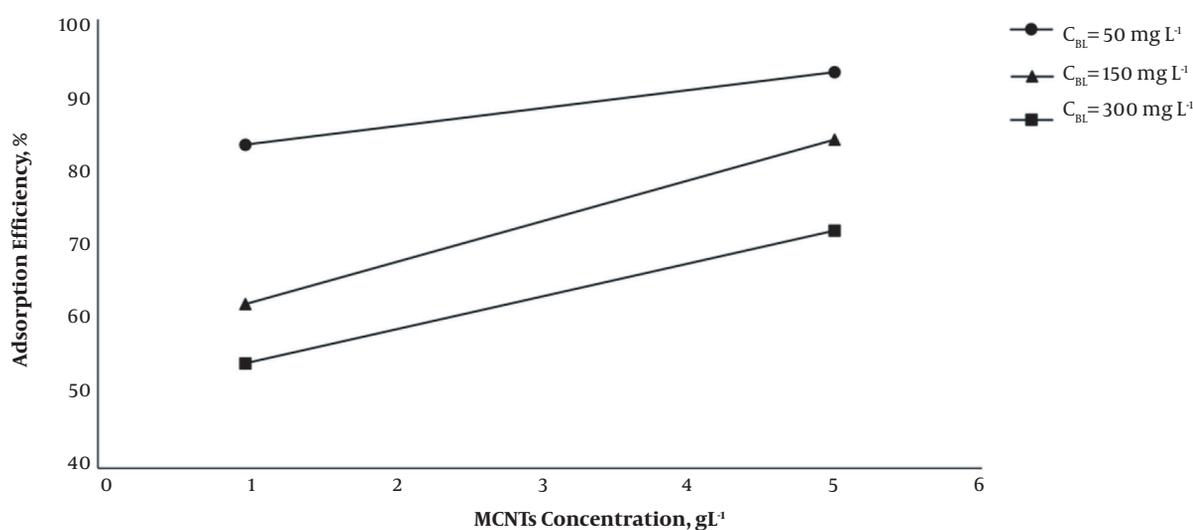
Figure 2. Effect of bromelain (BL) and magnetic carbon nanotubes (MCNTs) concentrations on adsorption efficiency

Table 1. Bromelain (BL) Adsorption Equilibrium Isotherm Parameters on Magnetic Carbon Nanotubes (MCNTs)

	Adsorption Isotherm Models					
Temperature (°C)	**Langmuir Model**			**Freundlich Model**		
	q_{max} (mg g^{-1})	K_L (L mg^{-1})	R^2	K_F ^{d} (mg g^{-1}) (L mg^{-1})$^{1/n}$	n	R^2
35	208.33	0.0208	0.9136	14.79	2.107	0.9887
50	156.25	0.0156	0.9242	10.33	2.164	0.9874

Abbreviations: q_{max}, maximum adsorption capacity; K_L, langmuir isotherm constant; n, intensity of the adsorption; K_F, Freundlich isotherm constant; R^2, correlation coefficient.
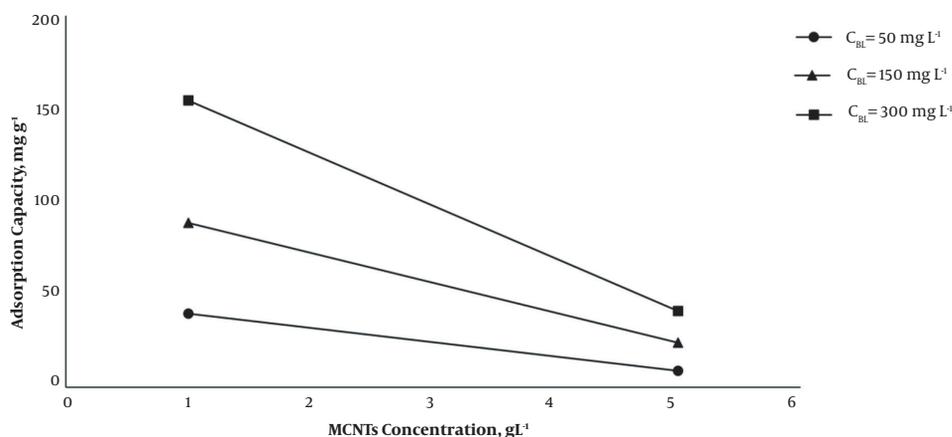
Figure 3. Effect of bromelain (BL) and magnetic carbon nanotubes (MCNTs) concentrations on adsorption capacity
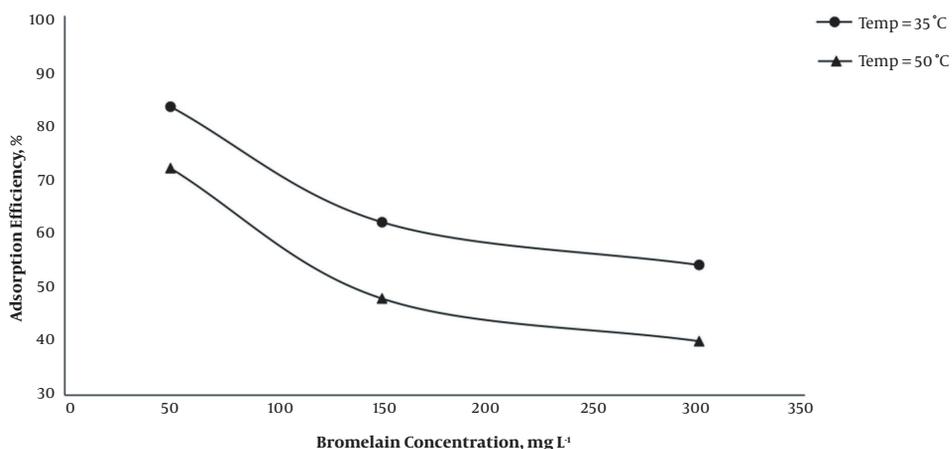
Figure 4. Effect of temperature on adsorption efficiency of bromelain (BL) from aqueous solutions

4.5. Adsorption Kinetics

The drug adsorption data at different contact times on MCNTs (CMCNTs = 1 g L^{-1}) were used to investigate the kinetic behavior of BL adsorption at 35°C and pH 7.2 - 7.4. The parameters for the pseudo-first and pseudo-second orders were calculated. For this purpose, the parameters of ln (q_e-q_t) and t/q_t were plotted in terms of t, and linear regression was performed (Table 2). The experimental data obtained from the adsorption experiments are in better agreement with the pseudo-second-order kinetic equation.

4.6. Cytotoxicity

The cytotoxicity level of BL and encapsulated BL in MNCTs against HT-29 cells was investigated by MTT assay (Figure 5A and B). BL at 10 μg mL^{-1} concentration significantly inhibited HT-29 growth, as shown in Figure 5. Also,

BL at 100 μg mL^{-1} demonstrated more than 50% reduction of cell viability after 24, 48, and 72 h. It was observed that after 72 h, the cells were highly vacuolated. However, encapsulated BL indicated the same decrease in cell viabilities only after 48 and 72h, which may be due to a gradual release of the drug over time.

5. Discussion

This study was performed on the adsorption of BL on MCNTs, and the function of this plant enzyme on inhibition of growth and proliferation of colon cancer cells. The results showed that the integration of MCNTs with BL improves the long-term effect of this enzyme. In other words, MCNTs release the drug more slowly and increase its effectiveness.

Table 2. Kinetic Parameters of the Bromelain (BL) Adsorption Process on Magnetic Carbon Nanotubes (MCNTs)

$q_{e(Experimental)}$ (mg g^{-1})	Kinetic Models					
	Pseudo-First-Order			Pseudo-Second-Order		
	$q_{e\,(Cal)}$ (mg g^{-1})	K_1 (min^{-1})	R^2	$q_{e\,(Cal)}$ (mg g^{-1})	K_2 [g (mg min)$^{-1}$]	R^2
41.62	71.73	0.075	0.956	44.24	0.0026	0.9975

Abbreviations: $q_{e(cal)}$, adsorption capacity at equilibrium; K_1, first-order rate constant; K_2, second-order rate constant; R^2, correlation coefficient.
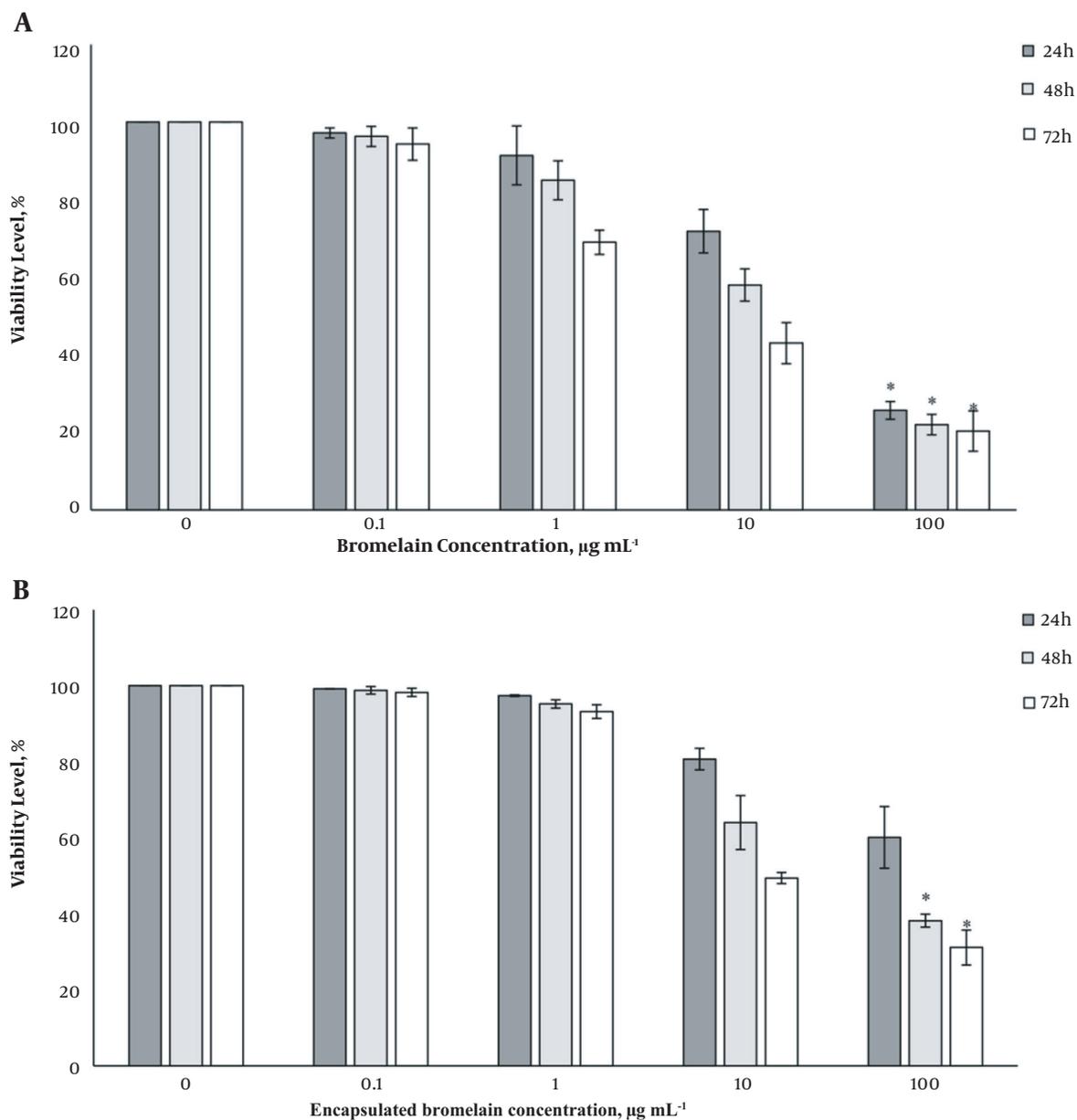
Figure 5. A, percent of cell viability at different concentrations of bromelain (BL); and B, encapsulated BL in magnetic carbon nanotubes (MCNTs) by MTT assay (*P < 0.001).

BL is an aqueous extract of pineapple containing a complex mixture of thiol proteases and non-proteasome components. Protease is a significant component of BL. It has been reported that the anticancer property of BL is mainly related to its protease components (3). In this study, it was attempted to investigate the anticancer properties of the BL enzyme alone and also in combination with MC-NTs. As it is known, MCNTs have some advantages in preventing the anticancer drug from degradation in the circulatory system and targeted delivery of an adequate drug to the tumor cells.

Evaluation of the efficacy of BL enzyme as an anticancer agent alone and in combination with other agents is often limited to preclinical trials (7, 8, 18). BL has been shown to selectively induce cell death in tumor cells by enhancing the effect of p53 and blocking the mitochondrial death pathway via enhancing Bax expression and cytochrome c release (19). Besides, BL reduces the activity of cell rescue regulators, such as Akt, which accelerates the death of cancer cells (20). In vitro studies have shown that the use of BL inhibits the growth of cancer cells in mice and reduces the capacity to spread cancer (21). BL also prevents cancer metastasis and adhesion of surface proteins that are required for adhesion, migration, and inflammation (22). Jaffe et al. showed that BL has an anticancer effect on human breast cancer cells of the GI101A class (23). Bhui et al. also showed that pretreatment with BL reduces the number and size of skin cancer cells in mice (24). Also, it has been recently shown that BL has an anti-proliferative effect on human A431 and murine A375 skin cancer cells (25). In 2013, Amini et al. investigated the effect of BL on four human colon cancer cell lines, including KATO-III, MKN45, HT29-5M21, and HT29-5F12. The results showed that the BL enzyme inhibited the proliferation of these cancer cells (26).

In 2015, Bhatnagar et al. synthesized a nanoparticle containing the BL enzyme and showed that it had higher anticancer activity than the BL itself, because of the increased release of the BL enzyme (5). In 2016, they developed a hyaluronic acid grafted PLGA copolymer, capable of targeting cancer cells as well as higher cellular uptake and cytotoxicity (7).

In 2012, Chen et al. functionalized SWCNTs using an ultrasonic DSPE-PEG2000-Amoni amine system. The results of this test showed that the encapsulating BL enzyme in SWCNTs has a significant effect on decreasing the growth and progression of breast cancer (27).

Our results demonstrated that at equilibrium in a solution containing 50 mg mL^{-1} of BL and 1 g L^{-1} MCNTs at 35°C, the amount of adsorbed BL was 41.62 mg g^{-1}. This number is very close to the number predicted by the pseudo-second-order kinetic model (44.24 mg). Therefore, it can be concluded that the dominant mechanism in the BL adsorption process on MCNTs is chemical adsorption. The pseudo-second-order kinetic model states that the two reactions in parallel were effective in the BL adsorption process on the MCNTs. The first reaction reaches equilibrium quickly, and the second lasts longer.

The results of the MTT assay indicated that BL had potent cytotoxicity at high concentrations (100 μg mL^{-1}) even after 24 h. However, regarding the encapsulated BL in MC-NTs, the viability rate decreased after 48 h, which shows a gradual release of the drug over time. As it is known, this type of drug release is favorable for cancer treatment. It is suggested that to obtain more definite results, more trials, especially in vivo experiments, are needed.

5.1. Conclusions

The optimized experimental parameters for BL adsorption were pH (7.2 - 7.4), adsorbent concentration (1g L^{-1}), temperature (35°C), contact time (90 min), and initial BL concentration (50 mg L^{-1}). The adsorption followed the Freundlich model better than the Langmuir model, and the Freundlich values indicated favorable adsorption of BL onto MCNTs. In addition, the adsorption followed second-order kinetics. Therefore, the predominant mechanism in the adsorption process on MCNTs is chemical adsorption. The decrease in adsorption capacity with temperature suggested the exothermic nature of adsorption.

The results indicated that MCNTs could be a potential effective adsorbent for the removal of BL from the solution. BL alone and in combination with MCNTs at 100 μg mL^{-1} concentration exhibited severe cytotoxicity effect on HT-29 cells. Although cellular viability in the presence of MC-NTs decreased slowly, the advantage of using MCNTs may be due to the slow delivery of encapsulated BL, which is favorable for cancer treatment.

Acknowledgments

Footnotes

References

1. Favoriti P, Carbone G, Greco M, Pirozzi F, Pirozzi RE, Corcione F. Worldwide burden of colorectal cancer: A review. *Updates Surg*. 2016;**68**(1):7–11. doi: 10.1007/s13304-016-0359-y. [PubMed: 27067591].

2. Gani MBA, Nasiri R, Hamzehalipour Almaki J, Majid FAA, Marvibaigi M, Amini N, et al. In vitro antiproliferative activity of fresh pineapple juices on ovarian and colon cancer cell lines. *Int J Pept Res Ther*. 2015;**21**(3):353–64. doi: 10.1007/s10989-015-9462-z.

3. Maurer HR. Bromelain: biochemistry, pharmacology and medical use. *Cell Mol Life Sci*. 2001;**58**(9):1234–45. doi: 10.1007/PL00000936. [PubMed: 11577981].

4. dos Anjos MM, da Silva AA, de Pascoli IC, Mikcha JM, Machinski MJ, Peralta RM, et al. Antibacterial activity of papain and bromelain on Alicyclobacillus spp. *Int J Food Microbiol*. 2016;**216**:121–6. doi: 10.1016/j.ijfoodmicro.2015.10.007. [PubMed: 26476327].

5. Bhatnagar P, Pant AB, Shukla Y, Chaudhari B, Kumar P, Gupta KC. Bromelain nanoparticles protect against 7,12-dimethylbenz[a]anthracene induced skin carcinogenesis in mouse model. *Eur J Pharm Biopharm*. 2015;**91**:35–46. doi: 10.1016/j.ejpb.2015.01.015. [PubMed: 25619920].

6. Dhandayuthapani S, Perez HD, Paroulek A, Chinnakkannu P, Kandalam U, Jaffe M, et al. Bromelain-induced apoptosis in GI-101A breast cancer cells. *J Med Food*. 2012;**15**(4):344–9. doi: 10.1089/jmf.2011.0145. [PubMed: 22191568].

7. Bhatnagar P, Pant AB, Shukla Y, Panda A, Gupta KC. Hyaluronic acid grafted PLGA copolymer nanoparticles enhance the targeted delivery of Bromelain in Ehrlich's Ascites Carcinoma. *Eur J Pharm Biopharm*. 2016;**105**:176–92. doi: 10.1016/j.ejpb.2016.06.002. [PubMed: 27287553].

8. Wei B, He L, Wang X, Yan GQ, Wang J, Tang R. Bromelain-decorated hybrid nanoparticles based on lactobionic acid-conjugated chitosan for in vitro anti-tumor study. *J Biomater Appl*. 2017;**32**(2):206–18. doi: 10.1177/0885328217715537. [PubMed: 28618976].

9. Arias S, Freire F, Quinoa E, Riguera R. Nanospheres, nanotubes, toroids, and gels with controlled macroscopic chirality. *Angew Chem Int Ed Engl*. 2014;**53**(50):13720–4. doi: 10.1002/anie.201406884. [PubMed: 25209219].

10. Porwal M. An overview on carbon nanotubes. *MOJ Bioequiv Bioavailab*. 2017;**3**(5):5–7. doi: 10.15406/mojbb.2017.03.00045.

11. Price PM, Mahmoud WE, Al-Ghamdi AA, Bronstein LM. Magnetic drug delivery: Where the field is going. *Front Chem*. 2018;**6**:619. doi: 10.3389/fchem.2018.00619. [PubMed: 30619827]. [PubMed Central: PMC6297194].

12. Ghorbani-Choghamarani A, Tahmasbi B, Noori N, Ghafouri-nejad R. A new palladium complex supported on magnetic nanoparticles and applied as an catalyst in amination of aryl halides, Heck and Suzuki reactions. *J Iran Chem Soc*. 2016;**14**(3):681–93. doi: 10.1007/s13738-016-1020-x.

13. Kakavandi B, Esrafili A, Mohseni-Bandpi A, Jonidi Jafari A, Rezaei Kalantary R. Magnetic Fe3O4@C nanoparticles as adsorbents for removal of amoxicillin from aqueous solution. *Water Sci Technol*. 2014;**69**(1):147–55. doi: 10.2166/wst.2013.568. [PubMed: 24434981].

14. Moussavi G, Alahabadi A, Yaghmaeian K, Eskandari M. Preparation, characterization and adsorption potential of the NH4Cl-induced ac-

15. tivated carbon for the removal of amoxicillin antibiotic from water. *Chem Eng J*. 2013;**217**:119–28. doi: 10.1016/j.cej.2012.11.069.

15. Ho YS, McKay G. Pseudo-second order model for sorption processes. *Process Biochem*. 1999;**34**(5):451–65. doi: 10.1016/s0032-9592(98)00112-5.

16. Ai L, Zhou Y, Jiang J. Removal of methylene blue from aqueous solution by montmorillonite/CoFe2O4 composite with magnetic separation performance. *Desalination*. 2011;**266**(1-3):72–7. doi: 10.1016/j.desal.2010.08.004.

17. Mahvi AH, Nabizadeh R, Rezaei Kalantary R, Rashidi AM, Nasseri S, Naghizadeh A. Adsorption kinetics and thermodynamics of hydrophobic natural organic matter (NOM) removal from aqueous solution by multi-wall carbon nanotubes. *Water Supply*. 2013;**13**(2):273–85. doi: 10.2166/ws.2013.018.

18. Chobotova K, Vernallis AB, Majid FA. Bromelain's activity and potential as an anti-cancer agent: Current evidence and perspectives. *Cancer Lett*. 2010;**290**(2):148–56. doi: 10.1016/j.canlet.2009.08.001. [PubMed: 19700238].

19. Debnath R, Majumder D, Singha AK, Ghosh D, Maiti D. Bromelain plus peroxidase from pine-apple induces apoptosis via mitochondrial dependent pathway in lymphoma cells. *Int J Pharm Sci Res*. 2018;**9**:4610–8.

20. Juhasz B, Thirunavukkarasu M, Pant R, Zhan L, Penumathsa SV, Secor EJ, et al. Bromelain induces cardioprotection against ischemia-reperfusion injury through Akt/FOXO pathway in rat myocardium. *Am J Physiol Heart Circ Physiol*. 2008;**294**(3):H1365–70. doi: 10.1152/ajpheart.01005.2007. [PubMed: 18192224]. [PubMed Central: PMC2581828].

21. Kalra N, Bhui K, Roy P, Srivastava S, George J, Prasad S, et al. Regulation of p53, nuclear factor kappaB and cyclooxygenase-2 expression by bromelain through targeting mitogen-activated protein kinase pathway in mouse skin. *Toxicol Appl Pharmacol*. 2008;**226**(1):30–7. doi: 10.1016/j.taap.2007.08.012. [PubMed: 17889918].

22. Lee JH, Lee JT, Park HR, Kim JB. The potential use of bromelain as a natural oral medicine having anticarcinogenic activities. *Food Sci Nutr*. 2019;**7**(5):1656–67. doi: 10.1002/fsn3.999. [PubMed: 31139378]. [PubMed Central: PMC6526645].

23. Paroulek AF, Jaffe M, Rathinavelu A. The effects of the herbal enzyme bromelain against breast cancer cell line GI101A. *FASEB J*. 2009;**23**(S1). doi: 10.1096/fasebj.23.1_supplement.LB18.

24. Bhui K, Prasad S, George J, Shukla Y. Bromelain inhibits COX-2 expression by blocking the activation of MAPK regulated NF-kappa B against skin tumor-initiation triggering mitochondrial death pathway. *Cancer Lett*. 2009;**282**(2):167–76. doi: 10.1016/j.canlet.2009.03.003. [PubMed: 19339108].

25. Bhui K, Tyagi S, Srivastava AK, Singh M, Roy P, Singh R, et al. Bromelain inhibits nuclear factor kappa-B translocation, driving human epidermoid carcinoma A431 and melanoma A375 cells through G(2)/M arrest to apoptosis. *Mol Carcinog*. 2012;**51**(3):231–43. doi: 10.1002/mc.20769. [PubMed: 21432909].

26. Amini A, Ehteda A, Masoumi Moghaddam S, Akhter J, Pillai K, Morris DL. Cytotoxic effects of bromelain in human gastrointestinal carcinoma cell lines (MKN45, KATO-III, HT29-5F12, and HT29-5M21). *Onco Targets Ther*. 2013;**6**:403–9. doi: 10.2147/OTT.S43072. [PubMed: 23620673]. [PubMed Central: PMC3633552].

27. Chen H, Ma X, Li Z, Shi Q, Zheng W, Liu Y, et al. Functionalization of single-walled carbon nanotubes enables efficient intracellular delivery of siRNA targeting MDM2 to inhibit breast cancer cells growth. *Biomed Pharmacother*. 2012;**66**(5):334–8. doi: 10.1016/j.biopha.2011.12.005. [PubMed: 22397761].